

메르캡탄(Mercaptan)-마이클 결합(Michael Coupling)과 ROMP: 기능성 나뭇가지형 폴리머의 공간 방해 효과에 대해 비교

Tong Wu[†], Maojie Xuan, Xingyou Wang, and Meina Liu[†]

School of Chemical and Environmental Engineering, Shanghai Institute of Technology
(2019년 1월 11일 접수, 2019년 5월 2일 수정, 2019년 9월 16일 채택)

Thiol-Michael Coupling and ROMP: Comparison of the Effects of Steric Hindrance with Functional Dendronized Polymer

Tong Wu[†], Maojie Xuan, Xingyou Wang, and Meina Liu[†]

*School of Chemical and Environmental Engineering, Shanghai Institute of Technology,
Shanghai, 100 Haiquan Road, China*

(Received January 11, 2019; Revised May 2, 2019; Accepted September 16, 2019)

Abstract: Dendronized *exo*-7-oxanorbornene monomers were synthesized and polymerized via thiol–Michael coupling and ring-opening metathesis polymerization. The polymerization rate was highly dependent on the steric hindrance of the terminal group. The space linker between the polymerizable group and dendron was a crucial factor. Ru-based kinetics was investigated using nuclear magnetic resonance (NMR), which showed that the monomer was completely converted to a generally narrow polydispersity material. The second generation of functional macromonomer was grafted from the first with a different linker length and consumed completely at 50 °C in toluene. Considering the properties of the space linker, we found that a short space linker of dendronized *exo*-7-oxanorbornene macromonomer leads to narrow molecular weight distributions of obtained dendronized polymers. This work provides a further understanding of the effect of steric hindrance on dendronized polymers, thereby allowing the development of functional materials.

Keywords: thiol–Michael, ring-opening metathesis polymerization, functional polymer, steric hindrance.

Introduction

Dendronized polymers, as important topological structures of branched polymer, have exhibited impressive advantages in terms of biology, medicine, catalysis, nanomaterials, and photoelectric materials in recent years.¹ Moreover, the highly branched and regular structures of dendronized polymers have unique physical and chemical properties, such as high rheological properties, good solubility and several modifiable terminal functional groups. These polymers are generally obtained from dendronized motifs through convergent and divergent methods.^{2,3} However, the synthesis process is immensely tedious that the deprotection and activation steps between each generation of dendronized polymers are

required.^{4,5} Recently, considerable effort has been devoted to macromonomer route research. Considering the facile and streamlined approach, the dendronized monomer with polymerizable groups is synthesized and polymerized via living polymerization.

Living polymerization is an efficient measure for realizing molecular design, and synthesizing a series of polymer materials with different structures and properties. Effective strategies such as atom transfer radical polymerization (ATRP), reversible addition–fragmentation chain transfer polymerization (RAFT), and ring-opening metathesis polymerization (ROMP), have been developed to design synthetic dendronized polymers. During ATRP, the removal process of transition metal complexes in polymers was cumbersome.^{6,7} Simultaneously, disulfide derivatives in RAFT may increase the toxicity of polymers.⁸ However, the initiation/propagation rate (k_i/k_p) ratio of ROMP increases with the catalyst development.^{9,10} Importantly, the degree of polymerization

[†]To whom correspondence should be addressed.
15395472710@163.com, ORCID 0000-0002-1736-8472
meina.liu@sit.edu.cn, ORCID 0000-0002-9928-2639
©2019 The Polymer Society of Korea. All rights reserved.

(DP) has a completely linear relationship with the consumed monomer.¹¹ Furthermore, the use of various thiol-based chemistries as tools for complex molecule synthesis, polymerization, and post-polymerization modification has received significant interest.¹²⁻¹⁴ For example, exclusively low levels of phosphine have been used as initiating species to catalyze the formation of the thiol–Michael adduct rapidly. On one hand, this approach can synthesize dendronized polymers with appropriate molecular weight distribution and high algebraic distribution; on the other hand, it can combine with “click” chemistry to produce multiple functional dendronized polymers.¹⁵⁻¹⁸

Recently, dendronized polymers have attracted significant attention due to their unique properties, specifically with the development of highly efficient active ROMP catalysts (Grubbs catalysts) and the diversification of polymerized monomers (cyclic olefins extended to cyclic monomers containing heteroatoms and polar functional groups). ROMP technology can prepare a dendronized polymer with controllable molecular weight via a macromolecular route.¹⁹ Schlüter *et al.* first used ROMP technology to prepare a dendronized polymer with a molecular weight of 216000 with RuCl_3 as catalyst.²⁰ With the limitation of RuCl_3 , the polymerization reaction did not exhibit the characteristic of living polymerization. Then, the same group reported the first case of active ROMP reaction. With $\text{RuCl}_2(=\text{CHPh})(\text{PCy}_3)_2$ as catalyst, they obtained a series of dendronized polymers with a molecular weight of 86900 by adjusting the ratio of the initial monomer and catalyst.²¹ Fréchet *et al.* successfully prepared high molecular weight dendronized polymers with biphenyl as the linking group containing second- and third-generation dendronized polymers with ruthenium-based catalyst, they confirmed dendronization through atomic force microscopy imaging.²² Weck and coworker found that an effective linker between the polymerizable group and the dendron can remarkably increase the polymerization rate.²³ Thus, as the degree increases, the monomer molecular chain elongates, and the terminal structure enlarges. These two factors have a potential effect during polymerization and an indispensable effect on polymer materials.

Herein, difunctional and tetrafunctional branched dendronized polymers were prepared via thiol–Michael coupling and ROMP. Among them, second-generation dendronized aromatic monomers were completely consumed in toluene at an elevated temperature and a topological material was obtained ($M_n = 23003$, PDI = 1.31). The steric hindrance effect observed

by NMR is evident during polymerization. As the end structure enlarges, the polymerization rate slows down, and further severe conditions are required to convert it fully. The space linker effect is also reflected. When the molecular chain shortened, we obtained dendronized polymers with a narrow PDI. The selected structures were used to produce functional materials for determining their polymerization performance.

Experimental

Materials. Anhydrous methanol, dichloromethane and tetrahydrofuran (THF) were purchased from Macklin Inc. Anhydrous toluene and triethylamine were used after redistillation. Other reagents were purchased from the Tansoole Co., Ltd (Shanghai, China) at the highest purity and used as received, unless noted otherwise.

Instrumentation. NMR spectra were recorded on a Bruker AVANCE III spectrometer at 500 MHz for hydrogen nuclei and 125 MHz for carbon nuclei in an appropriate deuterated solvent. Chemical shifts (δ) for ^1H NMR spectra were reported in parts per million (ppm). Data were presented as follows: chemical shift (multiplicity: s, singlet; d, doublet; dd, doublet of doublets; t, triplet; m, multiplet), coupling constants in Hz, and integration. THF size-exclusion chromatography (SEC) analyses were performed on a Shimadzu modular system comprising an autoinjector and a 5.0 mm bead-size guard column ($50 \times 7.5 \text{ mm}^2$) from Polymer Laboratories, followed by three linear PL columns and a differential refractive index detector using THF as the eluent at 40 °C with a flow rate of 1 mL min^{-1} . The system was calibrated with abovementioned linear polystyrene standards with narrow molecular weight distribution. High-resolution mass spectra (HRMS) were acquired on a Bruker Solaril X70 spectrometer with an Anaytica source.

Synthesis of 2-ene and 4-ene. Seven compounds were synthesized in good yields and characterized by NMR and HRMS (Scheme 1).

Synthesis of thiol–Michael Adducts. Table 1 shows a typical procedure for the thiol–Michael addition of a thiol, namely, R-SH, to 2-ene. A scintillation vial (20 mL capacity) was added with 2-ene (1.0 mmol, 1.0 equiv.) and the desired thiol (2.1 equiv.) dissolved in CH_2Cl_2 (2.0 mL). Dimethylphenylphosphine (Me_2PPh ; 5 mol%) was then added to the solution and the reaction was allowed to proceed at room temperature. The reaction was monitored by TLC and halted when the reagents were completely consumed. Solvent was removed

$J = 7.1$ Hz, 4H), 2.41 (dt, $J = 26.5, 9.0$ Hz, 4H), 1.66–1.55 (m, 4H), 1.41–1.31 (m, 4H), 1.27 (s, 3H). ^{13}C NMR (125 MHz, CDCl_3 , ppm) $\delta = 176.22, 172.49, 170.96, 136.43, 122.79$ – 106.15 (m, CF2, CF3), 80.86, 65.41, 65.06, 47.31, 46.16, 38.56, 34.26, 31.98, 31.82, 31.64, 29.59, 28.20, 27.28, 26.89, 25.99, 25.19, 22.64, 17.77. ^{19}F NMR (470 MHz, CDCl_3 , ppm) $\delta = -80.80$ (m, 6F), -114.34 (m, 4F), -121.40 to -124.25 (m, 12F), -126.16 (m, 4F). HRMS: calculated for $\text{C}_{41}\text{H}_{41}\text{F}_{26}\text{NO}_9\text{S}_2$ [$\text{M}+\text{H}^+$] 1249.8555, found 1249.8557.

(((2-(((6-((3aR,7aS)-1,3-dioxo-1,3,3a,4,7,7a-hexahydro-2H-4,7-epoxyisoindol-2-yl)hexyl)oxy) carbonyl)-2-methylpropane-1,3-diol)bis(oxy))bis (carbonyl))bis(2-methylpropane-2,1,3-triyl) tetrakis(3-(benzylthio)prop-anoate) (**M23**)

G2'' (0.913 g, 1.1 mmol) and benzyl mercaptan (646 μL , 5.5 mmol) were reacted for 6 h. The adduct was isolated as a colorless syrup in a 60% yield (0.825 g). ^1H NMR (500 MHz, CDCl_3 , ppm) $\delta = 7.28$ (d, $J = 31.0$ Hz, 20H), 6.51 (s, 4H), 5.26 (s, 4H), 4.26 (d, $J = 3.2$ Hz, 26H), 4.10–4.08 (m, 5H), 3.72 (d, $J = 1.4$ Hz, 18H), 3.47 (s, 5H), 2.83–2.80 (m, 14H), 2.65 (d, $J = 5.1$ Hz, 8H), 1.62–1.56 (m, 10H), 1.24 (s, 11H). ^{13}C NMR (125 MHz, CDCl_3 , ppm) $\delta = 176.29, 172.09, 171.25, 169.70, 138.01, 136.54, 128.85, 128.56, 127.11, 80.92, 65.70, 65.46, 65.17, 47.39, 46.59, 46.36, 38.88, 38.69, 37.34, 36.24, 34.23, 28.32, 27.36, 26.12, 25.32, 17.84$. HRMS: calculated for $\text{C}_{69}\text{H}_{83}\text{NO}_{17}\text{S}_4$ [$\text{M}+\text{H}^+$] 1326.6531, found 1326.6536.

Typical Procedure for the Online Monitoring of ROMP of the Thiol–Michael Adducts via ^1H NMR Spectroscopy. In 20 mL glass bottles, monomers and catalysts (Grubbs, the ratio being dictated by the targeted molecular weight) were dissolved in solvent and then stirred under nitrogen protection. The polymerization inhibitor (ethyl vinyl ether) was added to the solution and stirred for 30 min. The conversion was monitored by comparing the ratio of the integrals of the polymeric to monomeric ene peaks *versus* time with NMR.

Results and Discussion

Thiol–Michael Coupling. We selected poly(exo-7-oxanorbornene) as the polymerizable backbone and a polyester-based structure. Exo-7-oxanorbornene was linked to the backbone with various lengths of carbon chains. Thiol was grafted onto the end of the branched macromolecule via Michael addition of thiol olefins to obtain functional monomers. This work aimed to compare the effect of steric hindrance with functional groups. We initially targeted the difunctional and tetrafunctional derivatives of diacrylate and tetraacrylate functional den-

dron species that would serve as common substrates in ROMP.

As outlined in Scheme 1, 2-ene and 4-ene were prepared via multistep procedures. They were synthesized in a four-step process involving the initial preparation of 2,2,5-trimethyl-1,3-dioxane-5-carboxylic acid that was subsequently reacted with alcohol **A''** in a carbodiimide coupling to provide the protected diol **B''**. Treatment of **B''** with Dowex- H^+ generated the corresponding free diol **C''**. **C''** serves as a common precursor to **G1''** and **G2''** because it can be acylated with acryloyl chloride, to produce **G1''** or reacted with 2,2,5-trimethyl-1,3-dioxane-5-carboxylic acid in another carbodiimide-mediated esterification to provide protected tetraol **D''**, which generates free tetraol **E''** after treatment with Dowex- H^+ . Esterification of tetraol (**E''**) with acryloyl chloride, mediated by pyridine, provides target tetraacrylate **G2''**.²⁴ Pyridine has excellent performance in esterifying multiple sites. In all instances, the yields of various synthetic steps were good to excellent, and all products were characterized using standard methods. As an example, Figure 1 shows the ^1H NMR spectrum, recorded in CDCl_3 , of diacrylate dendron monomers **G1''** and **G2''** with peak assignments confirming their structure.

2-ene and 4-ene converted numerous thioether adducts via Me_2PPh -mediated thiol–Michael coupling reactions (Tables 1 and 2, respectively).²⁵ Seven mercapto compounds were 1H, 1H,2H,2H-perfluorodecanethiol, the siloxy species 3-mercaptopropyltriethoxysilane, benzyl mercaptan, methyl 3-mercaptopropionate, mercaptopropyl-isobutyl-POSS, 3-mercaptopropanol, and acetyl-thiol-glucose. In all instances, the target adducts were isolated in good to excellent yields, and their

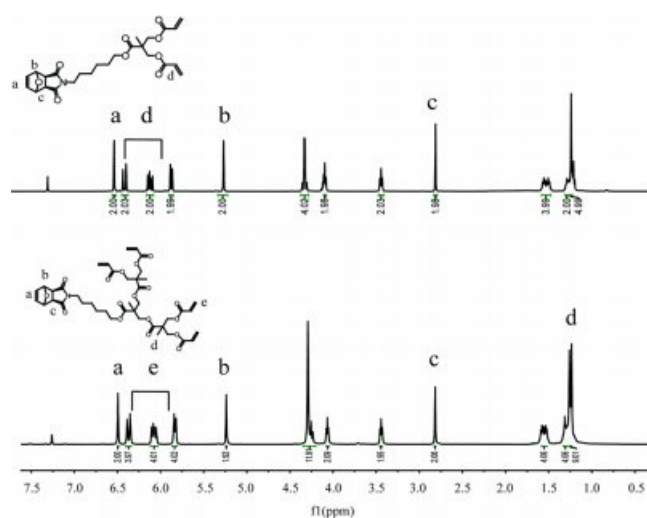


Figure 1. ^1H NMR spectrum, recorded in CDCl_3 , of functional exo-7-oxanorbornene monomers **G1''** and **G2''**.

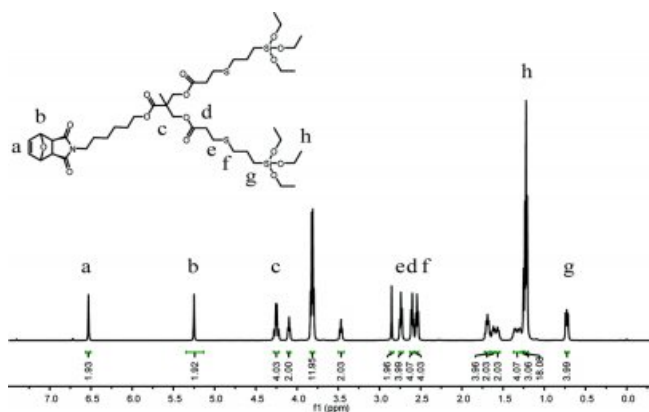


Figure 2. ^1H NMR spectrum, recorded in CDCl_3 , of the bis siloxane functional dendron monomer with several key peak assignments.

structures were confirmed using a combination of NMR spectroscopy and HRMS. In addition, the tetrafunctional–aromatic adduct was prepared from the reaction of 4-ene with benzyl mercaptan. The tetrafunctional thioether adduct was isolated in a 60% yield. However, other thiols have a Michael addition reaction with 4-ene, leading to the low isolated yield. As a representative example, Figure 2 shows the ^1H NMR spectrum for silicone functional dendron species **M12**. Several points are worth highlighting. Importantly, the alkane resonance associated with methyl was clearly visible at $\delta = 1.21$ ppm (labelled h). A simple ratio of these signals with a or b (the vinylic Hs associated with the oxanorbornene and the corresponding allylic Hs at the bridgehead O) confirmed the structure. In addition, we observed two sets of peaks at $\delta = 2.74$ and 2.54 ppm, which were closely related to the bridging of the bridged sulfur bonds between the siloxane functional groups and olefins. All peaks integrated in a ratio expected for the target structure.

ROMP. With a small library of thioether functional 2-ene derivatives available, we evaluated the capability to homopolymerize substrates with Grubbs' [Ru]-based ROMP initiators. In initial screenings, we intentionally targeted low molecular weight homopolymers (target $M_n = 10$ kDa) to determine the capability of the highly functional and sterically bulky monomers to undergo polymerization. Figure 3 shows the representative ^1H NMR and kinetic conversion data for the homopolymerization (target $M_n = 10$ kDa) of the dendron monomers derived from difunctional derivative.

The reaction in Figure 3(A) shows the homopolymerization of the aromatic dendron monomer **M8**. This example indicates that the double bond of the 7-oxanorbornene was broken to

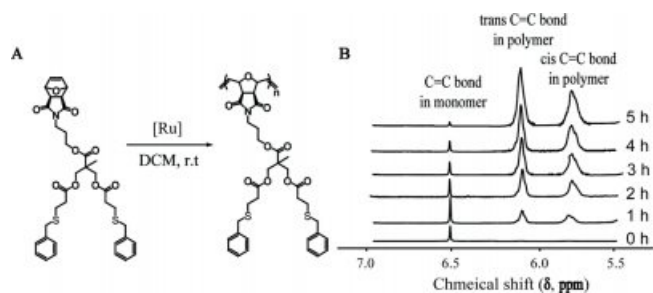


Figure 3. (A) Representative monomer catalyzed by Grubbs catalyst to obtain the dendronized polymers in DCM; (B) conversion *versus* time profiles generated from the NMR data for the homopolymerization of the benzyl functional dendron monomers, also highlighting the effect of the [Ru] initiator.

form a chain structure under the Ru-based catalysis. Figure 3(B) presents a series of selected ^1H NMR spectra, each of which was directly recorded in the spectrometer for the homopolymerization of the aromatic dendron monomer. ^1H NMR spectroscopy is a convenient technique that can be applied following monomer consumption in ROMP. This fact stems from the distinct chemical shift of the vinyl resonance associated with the monomer, compared with the cis/trans vinylic bonds in the resulting polymer.^{26,27} We can clearly observe the monomer vinyl resonance above $\delta = 6.5$ ppm, a signal that decreases in intensity with the an increase in polymerization time. The two broad resonances associated with the polymer backbone appear between $\delta = 5.8$ ppm and $\delta = 6.2$ ppm, wherein an increase in intensity is associated with an increase in polymerization time. A simple ratio of the integrals associated with these resonances allows the conversion to be determined at any given time (specifically at greater than 95% for the aromatic adduct after 6 h), as well as the generation of the kinetic conversion *versus* time profiles.

Table 3 shows examples of such profiles and several features that are worth highlighting. First, the capability of preparing polymers with a high average DP is desirable for demonstrating the validity of the dendron monomer approach detailed herein. The dual functional dendron monomers are susceptible to homopolymerization with Grubbs' I and III initiators, albeit with relatively low DP. Then, we evaluated the capability to prepare homopolymers with significantly high DP. For this series of experiments, we focused exclusively on the 7-oxanorbornene derivative of the Grubbs' III initiator with polymerizations performed in different environments. Table 2 presents a summary of the theoretical targeted M_n values, together with the target DP values at quantitative conversion and the

Table 3. Summary of Reaction Conditions, Polymerization Time, Measured Average Molecular Weights and Dispersity Values for the Homopolymerization of Monomers Derived from 2-ene with the [Ru] Catalyst (Theoretical Average Molecular Weights = 10 kDa)

Entry	Monomer	[Ru]	M/I	Solvent and Temp.	Time (h)	Conv. ^a (%)	M_w^b (kDa)	M_n^b (kDa)	PDI ^b
1	M1	G1	8.36	DCM, r.t	6	100	8849	7871	1.12
2	M2	G1	8.25	DCM, r.t	6	100	7527	6461	1.16
3	M3	G1	8.00	DCM, r.t	6	100	10625	9054	1.17
4	M4	G1	14.67	DCM, r.t	6	100	4915	3900	1.26
5	M5	G1	14.33	DCM, r.t	6	100	7686	6075	1.26
6	M6	G1	13.59	DCM, r.t	6	100	9816	7326	1.34
7	M7	G1	10.82	DCM, r.t	6	76	68664	50488	1.36
8	M8	G1	10.63	DCM, r.t	6	72	86784	54926	1.58
9	M9	G1	10.22	DCM, r.t	6	58	85647	68374	1.25
10	M7	G3	10.82	THF, 50 °C	3	100	97764	94000	1.04
11	M8	G3	10.63	THF, 50 °C	3	100	89634	80030	1.12
12	M9	G3	10.22	THF, 50 °C	3	100	106830	98916	1.08
13	M10	G3	14.25	DCM, r.t	6	100	8536	7124	1.19
14	M11	G3	13.93	DCM, r.t	6	100	7353	5600	1.31
15	M12	G3	13.23	DCM, r.t	6	100	9923	7083	1.40
16	M10	G3	14.25	Tol, r.t	3	100	10149	8528	1.19
17	M11	G3	13.93	Tol, r.t	3	100	10289	8058	1.27
18	M12	G3	13.23	Tol, r.t	3	100	10686	8283	1.29
19	M13	G3	4.51	DCM, r.t	6	100	10800	9075	1.19
20	M14	G3	4.46	DCM, r.t	6	100	11256	9226	1.22
21	M15	G3	4.38	DCM, r.t	6	100	11985	8812	1.36
22	M16	G3	8.60	DCM, r.t	6	100	4762	4369	1.09
23	M17	G3	8.49	DCM, r.t	6	100	4980	4517	1.10
24	M18	G3	8.24	DCM, r.t	6	100	7544	6149	1.23
25	M19	G3	15.98	THF, 50 °C	6	82	7091	5812	1.22
26	M20	G3	15.34	THF, 50 °C	6	77	7156	5679	1.26
27	M21	G3	14.49	THF, 50 °C	6	65	8458	5874	1.44

^aDetermined using NMR. ^bDetermined using SEC.

SEC-measured number- and weight-average molecular weights and PDI.

Fluorinated derivative (Entries 1–3) and ester-containing chain derivative (Entries 4–6) could be polymerized for quantitative conversion with Grubbs' I catalyst within *ca* 6 h to generate a homopolymer with the SEC measurement. The reason is that they are all straight chain structures with small steric hindrance. Hence, the polymerization conditions are considerably easier than those of other derivatives. By contrast, the use of Grubbs' I initiator with trimethoxysilane derivatives (Entries 7–9) resulted in an incomplete conversion with the siloxy derivative reaching a maximum measured conversion of *ca* 50%. However, under these circumstances, near-quantitative conversion was achieved by substituting the Grubbs' I species with the Grubbs' third-generation initiator, namely,

$\text{RuCl}_2(3\text{-BrPy})_2(\text{ImMesH}_2)\text{CHPh}$ (Grubbs' III; data are shown for the trimethoxysilane, aromatic, POSS, and the sugar derivatives) (Entries 10–24). Consistent with previous reports on the enhanced catalytic efficiency of Grubbs' III species over Grubbs' I or II species,^{28,29} the polymerizations were rapid with the aromatic derivative and the POSS derivative reached >95% conversion within *ca* 6 h (Entries 13–21).

The steric hindrance effect already became apparent. Special structures, such as sugar structure, and aromatic nucleus, etc. caused a low reactivity. In the polymerization of bis siloxy derivative, solvents must be changed from CH_2Cl_2 to THF to facilitate high conversions. In addition, the reaction temperature must be raised from room temperature to 50 °C. The polymerization time was shortened by 3 h (Entries 7–12), and the polymer solubility in the organic solvent after sedimen-

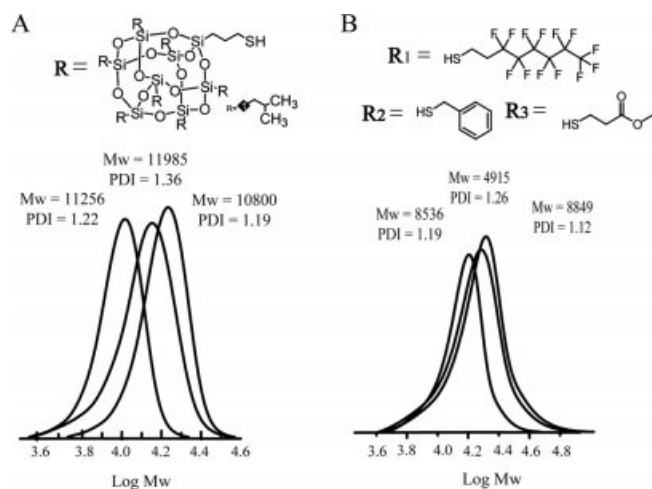


Figure 4. SEC traces for (A) the products from the homopolymerization of POSS derivatives with various linker lengths (middle, linker length $n = 2$; right, linker length $n = 3$; left, linker length $n = 6$); (B) the products from the linker length $n = 2$ and homopolymerization of various terminal groups (left, 1H,1H,2H,2H-perfluorodecanethiol; middle, benzyl mercaptan; and right, methyl 3-mercaptopropionate).

tation treatment was poor. After SEC testing, the test molecular weight greatly differed from the theoretical molecular weight because the derivative end of silicon oxygen bonds was hydrolytically broken in air to form a crosslinked network structure.³⁰ The obtained polymer had certain tensile and thermal stability and a certain degree of ductility, which provided a broad prospect for the application of such derivatives in materials.³¹

Aromatic derivatives had a wide value of PDI under the same conditions, but they had suitable values in toluene at

room temperature. Then, the polymerization of bis aromatic derivatives was more controlled in toluene than in dichloromethane at room temperature (Entries 16–18). Furthermore, the reaction time was shortened by 3 h. The performance of difunctional monomer with hydroxyl was unsatisfactory in THF at an elevated temperature (Entries 25–27). In general, the characteristics of the end group have an indispensable influence on the reaction environment (catalyst, solvent and temperature).

The terminal group is POSS. With the growth of the linker group (alkanolamine), the molecular weight shows a significant increase, but the molecular weight distribution widens, as presented in Figure 4(A). The longer the space linker length of the dendritic polymer with the same end group, the wider the molecular weight distribution. Hence, derivatives with the [Ru] catalyst had a broad molecular weight distribution, as shown in Table 3. Considering the effect of steric hindrance on the polymerization of 7-oxa-norbornene ROMP from Figure 4(B), when the linking group is ethanolamine, the greater the steric hindrance of the terminal group, the greater the PDI. The dendronized polymer with a chain end had a narrow molecular weight distribution (Entries 1, 4, and 10). A large fluorine content could cause size and phase separation. The molecular weight distribution of the end straight chain structure is superior to that of the end aromatic or end cage groups (Entries 3, 9, and 21).

As shown in Table 4 and Figure 5(A), the reaction time was prolonged with the increase in molecular weight (Entries 1–3). Moreover, different linker lengths led to a large difference in the conversion rate of monomers and affected the molecular weight distribution. The monomer molecular chain length

Table 4. Summary of Reaction Conditions, Polymerization Time, Conversion Rate, Measured Average Molecular Weights, and Dispersity Values for the Homopolymerization of Monomers Derived from Difunctional Derivatives with Grubbs' III Catalyst (Theoretical Average Molecular Weights = 30 kDa)

Entry	Monomer	M/I	Solvent and Temp.	Time (h)	Conv. ^a (%)	M_w^b (kDa)	M_n^b (kDa)	PDI ^b
1	M1	25.09	THF, 50 °C	12	86	26596	23330	1.14
2	M2	24.76	THF, 50 °C	12	77	26692	22432	1.19
3	M3	24.00	THF, 50 °C	12	61	27543	22762	1.21
4	M4	44.00	Tol, 50 °C	3	100	35160	26637	1.32
5	M5	42.99	Tol, 50 °C	3	98	41407	29363	1.41
6	M6	40.77	Tol, 50 °C	3	95	48333	32658	1.48
7	M10	42.74	Tol, 50 °C	3	100	22016	17066	1.29
8	M11	41.78	Tol, 50 °C	3	100	20975	16259	1.29
9	M12	39.68	Tol, 50 °C	3	100	22781	14603	1.56

^aDetermined using NMR. ^bDetermined using SEC.

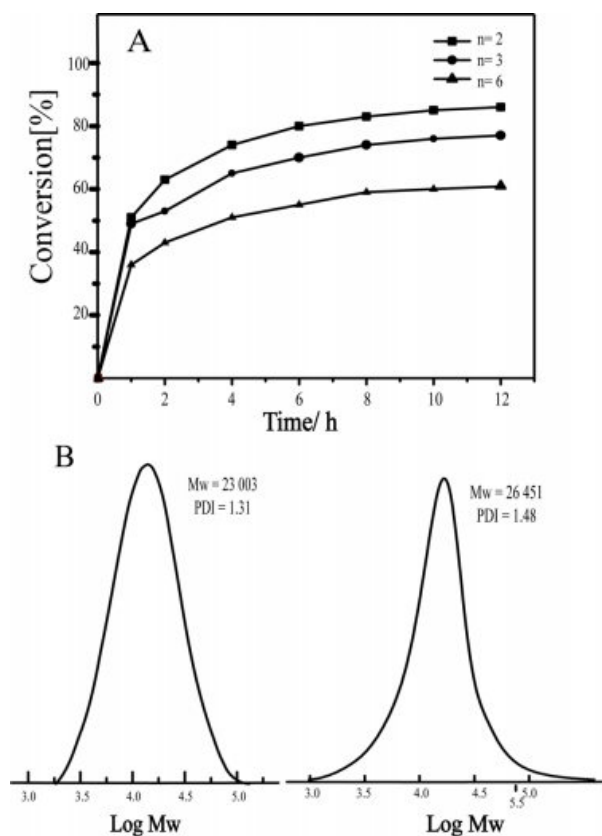


Figure 5. (A) Conversion of difunctional fluorinated derivatives over time under theoretical molecular weight = 30000; (B) SEC traces for the product from the homopolymerization of the tetrafunctional-aromatic derivatives with Grubbs' III initiator in Tol at 50 °C. Left: linker length = 2. Right: linker length = 6.

increased and the polydispersity enlarged. When THF was used as solvent at a heating condition of 50 °C, the molecular weight distribution was broad (>1.5) for aromatic and ester chain derivatives. Subsequently, THF was replaced with toluene under various heating conditions (Entries 4–9). The reaction time was considerably shortened, the conversion was almost complete, and the molecular weight distribution was within an acceptable range.

The reaction site of the tetrafunctional derivative was more than that of the difunctional derivative. After Michael addition reaction, the products of different functional derivatives were produced, and the polarities were similar, resulting in a low separation yield. In a series of addition reactions, the isolated yield of aromatic derivatives was the highest ($>70\%$). However, other thiol compounds, such as methyl 3-mercaptopropionate and 1H,1H,2H,2H-perfluorodecanethiol, were challenging for separation with low yields. Through computer simulation,

we found that the steric hindrance energy of different adducts (one-, two-, and three-adduct products) varied greatly. The reason may be the low yield of the target product.³² The benzyl group was in a planar configuration, whereas the other two were in a chain structure, which was prone to torsional winding. The homopolymerization of this tetrafunctional species proved to be challenging. As the tetrafunctional molecular weight was considerably greater than the difunctional molecular weight, for ROMP homopolymerization, the theoretical molecular weight set to 30000 required a complete 12 h conversion in THF 50 °C with Grubbs' III catalyst, but $PDI >2.5$. Furthermore, after replacing the solvent with toluene, in 50 °C heating for 3 h, the conversion was complete and an acceptable PDI was obtained. The effect of chain length was consistent with the difunctional derivatives. As the chain length increased, the obtained molecular weight distribution widened. However, for a high molecular weight, any improved reaction conditions were not found.

Conclusions

We reported the synthesis of two types of multifunctional dendron acrylic *exo*-7-oxanorbornene monomers, namely, difunctional and tetrafunctional derivatives. 2-ene and 4-ene served as precursors to thioether-based functional dendron monomers via straightforward nucleophilic thiol–Michael conjugation between acrylic groups and various functional thiols, such as siloxane and aromatic thiols. [Ru] kinetics was demonstrated by NMR, and the monomer was completely converted to a material with a generally narrow polydispersity under appropriate conditions. The synthesis and homopolymerization of aromatic derivatives derived from 4-ene proved to be challenging, but such derivatives were successfully polymerized with Grubbs' III initiator in toluene at elevated temperature. The end group affected the functional dendronized polymer. The shorter the space linker of the dendronized *exo*-7-oxanorbornene macromonomer, the narrow molecular weight distributions of the obtained dendronized polymers.

Acknowledgements: This work was supported by the National Natural Science Foundation of China (No. 21604056), Natural Science Foundation of Shanghai (No. 16ZR1435600), State Key Laboratory of Molecular Engineering of Polymers (No. K2017-16), Key Laboratory of Synthetic, and Self-Assembly Chemistry for Organic Functional Molecules (No. K2017-7).

References

1. K. Liu, Z. Xu, and M. Yin, *Prog. Polym. Sci.*, **46**, 25 (2015).
2. R. H. E. Hudson and M. J. Damha, *J. Am. Chem. Soc.*, **115**, 2119 (1993).
3. L. Song, Q. Jiang, Z.-G. Wang, and B. Ding, *ChemNanoMat.*, **3**, 713 (2017).
4. Y. Shi, W. Zhu, and Y. Chen, *Macromolecules*, **46**, 2391 (2013).
5. A. Carlmark, C. Hawker, A. Hult, and M. Malkoch, *Chem. Soc. Rev.*, **38**, 352 (2009).
6. N. V. Tsarevsky, S. R. Woodruff, and P. J. Wisian-Neilson, *J. Chem. Ed.*, **93**, 1452 (2016).
7. H. Lee, *Polym. Korea*, **39**, 165 (2015).
8. D. Sprouse and T. M. Reineke, *Biomacromolecules*, **15**, 2616 (2014).
9. K. O. Kim, S. Shin, J. Kim, and T.-L. Choi, *Macromolecules*, **47**, 1351 (2014).
10. A. A. Antonov, N. V. Semikolenova, V. A. Zakharov, W. Zhang, Y. Wang, W.-H. Sun, E. P. Talsi, and K. P. Bryliakov, *Organometallics*, **31**, 1143 (2012).
11. M. Liu, B. H. Tan, R. P. Burford, and A. B. Lowe, *Polym. Chem.*, **4**, 3300 (2013).
12. L. Zhu, T. J. Zimudzi, N. Li, J. Pan, B. Lin, and M. A. Hickner, *Polym. Chem.*, **7**, 2464 (2016).
13. A. Dondoni and A. Marra, *Chem. Soc. Rev.*, **41**, 573 (2012).
14. M. Liu, J. van Hensbergen, R. P. Burford, and A. B. Lowe, *Polym. Chem.*, **3**, 1647 (2012).
15. J. A. van Hensbergen, M. Liu, R. P. Burford, and A. B. Lowe, *J. Mater. Chem. C*, **35**, 693 (2015).
16. K. Matyjaszewski, *Macromolecules*, **45**, 4015 (2012).
17. W. D. Mulhearn and R. A. Register, *ACS Macro Lett.*, **6**, 112 (2017).
18. C. E. Wang, P. S. Stayton, S. H. Pun, and A. J. Convertine, *J. Control. Release*, **219**, 345 (2015).
19. W. Wieczorek, A. Zalewska, D. Raducha, Z. Florjańczyk, J. R. Stevens, A. Ferry, and P. Jacobsson, *Macromolecules*, **29**, 143 (1996).
20. V. Percec and D. Schlueter, *Macromolecules*, **30**, 5783 (1997).
21. S. Rajaram, T.-L. Choi, M. Rolandi, and J. M. J. Fréchet, *J. Am. Chem. Soc.*, **129**, 9619 (2007).
22. K. O. Kim and T.-L. Choi, *ACS Macro Lett.*, **1**, 445 (2012).
23. H. Jung, T. P. Carberry, and M. Weck, *Macromolecules*, **44**, 9075 (2011).
24. M. Liu, R. P. Burford, and A. B. Lowe, *Polym. Int.*, **63**, 1174 (2014).
25. J. Yamuna, T. Siva, S. S. S. Kumari, and S. Sathiyarayanan, *RSC Adv.*, **6**, 79 (2016).
26. D. A. Rankin, S. J. P'Pool, H.-J. Schanz, and A. B. Lowe, *J. Polym. Sci., Part A: Polym. Chem.*, **45**, 2113 (2007).
27. M. A. Tallon, Y. Rogan, B. Marie, R. Clark, O. M. Musa, and E. Khosravi, *J. Polym. Sci., Part A: Polym. Chem.*, **52**, 2477 (2014).
28. T.-L. Choi and R. H. Grubbs, *Angew. Chem. Int. Ed.*, **42**, 1743 (2003).
29. G. C. Vougioukalakis and R. H. Grubbs, *Chem. Rev.*, **110**, 1746 (2010).
30. F. Mangolini, J. Hilbert, J. B. McClimon, J. R. Lukes, and R. W. Carpick, *Langmuir*, **34**, 2989 (2018).
31. T. Ha, I. Hwang, Y. Bang, K. Kim, J. Kim, S. Kim, and K. Kim, *Polym. Korea*, **40**, 992 (2016).
32. Z. Zhao, S. Chen, J. W. Y. Lam, C. K. W. Jim, C. Y. K. Chan, Z. Wang, P. Lu, C. Deng, H. S. Kwok, Y. Ma, and B. Z. Tang, *J. Phys. Chem. C*, **114**, 7963 (2010).